

Coherence in Arrays of Spin-Torque Nano Oscillators

K. Beauvais*, J. Turtle*, A. Palacios*, V In** and P Longhini**

* Nonlinear Dynamics Group, San Diego State University
San Diego, CA, USA, james.a.turtle@gmail.com

** Space and Naval Warfare Systems Center Pacific, San Diego, USA

ABSTRACT

In this work we explore the use of Spin-Torque Nano Oscillators (STNO)s to build a voltage oscillator in the microwave range. STNOs are quite small—on the order of 100 nm—and frequency agile. We attempt to increase power output by investigating the dynamics of a system of electrically-coupled STNOs. Bifurcation diagrams are generated to better understand the dynamics of 2 coupled STNOs. We then computationally calculate the coherence parameter on a two parameter grid to study synchronization for larger N .

Keywords: synchronization, dynamics, coherence, bifurcation, oscillations

1 INTRODUCTION

Spintronics is a developing field of electronics that seeks to leverage the characteristics of electron spin. Specifically, we are interested in the magnetization or magnetic moment within a ferromagnetic layer. A Spin Torque Nano-Oscillator (STNO) is a ferromagnet-based electronics component. Under certain conditions the magnetization will precess, causing the STNO's resistance to oscillate. Based on this oscillating resistance, an STNO can be utilized as a microwave-frequency voltage oscillator. Some of the traits of STNOs include: small size ($\sim 100\text{nm}$), more robust materials than semiconductors, and tunable over a large frequency range. However, the power output produced in experiments is very small; on the order of 100 nW [1]. To be viable as an electronics component, a power output of at least 1 mW is likely required [2]. One method for increasing power is to couple many STNOs in a single circuit. However, attempts to synchronize even two oscillators have proven difficult [3]. We study the dynamics of coupled STNOs to determine conditions that produce synchrony in the system. In this paper we first analyze the equations for $N = 2$ oscillators arrayed in series. Simplifying assumptions are made to reduce expression complexity and facilitate further analysis. We then consider coherence calculation as a computational method to characterize the synchronization properties of larger systems ($N > 2$).

2 MODEL

The magnetic moment or magnetization of a magnetic material is caused by electron spin and orbit. Magnetization in the free ferromagnetic layer of an STNO is described by the Landau-Lifshitz equation with Gilbert damping and Slonczewski-Berger spin-torque term (LLGS) [4]–[8]

$$\frac{d\mathbf{m}}{dt} = \underbrace{-\gamma\mathbf{m} \times \mathbf{H}_{\text{eff}}}_{\text{precession}} + \underbrace{\lambda\mathbf{m} \times \frac{d\mathbf{m}}{dt}}_{\text{damping}} - \underbrace{\gamma\mu I \mathbf{m} \times (\mathbf{m} \times \mathbf{M})}_{\text{spin transfer torque}}. \quad (1)$$

Here \mathbf{m} represents the magnetization of the free ferromagnetic layer in Cartesian coordinates and γ is the gyromagnetic ratio. λ serves as the magnitude of the damping term. Spin-torque is the result of polarized electrons entering the free layer. The fixed or polarizing layer has magnetization direction \mathbf{M} . Without loss of generality, μ is assumed to equal 1. This makes the electric current I unit-less, but does not effect the dynamics. \mathbf{H}_{eff} is the sum of several factors that can be effectively represented as external fields. The factors that we consider in this fashion are: uniaxial anisotropy, demagnetization and the actual external (applied) field.

The LLGS preserves the magnitude $\|\mathbf{m}\|_2$, thus modeling magnetization direction on the surface of a sphere. As in [9] a complex stereographic projection is used to project the domain from the surface of a sphere to the stereographic plane

$$\begin{aligned} \dot{z}_j = & \frac{\gamma(1+i\lambda)}{1+\lambda^2} \left[ih_{a3}z_j + \frac{h_{a2}}{2}(1+z_j^2) + i\kappa \frac{1-|z_j|^2}{1+|z_j|^2} z_j \right. \\ & - \mu I_{\text{dc}} \beta_{Rc} \left(z_j + \beta_{\Delta R} \sum_{k=1}^N \frac{1-|z_k|^2}{1+|z_k|^2} z_j \right) \\ & - \frac{4\pi i S_0}{1+|z_j|^2} \left(\frac{N_1 - N_2}{2} (z_j^3 - \bar{z}_j) \right) \\ & \left. + \left(1 - \frac{3N_1 + 3N_2}{2} \right) (z_j - z_j|z_j|^2) \right], \quad (2) \end{aligned}$$

thus reducing the dimension of each oscillator by one. Here I_{dc} is the constant input-current to a series-arrayed circuit (see [9]). We have chosen the uniaxial anisotropy to be in the z -direction and with magnitude κ . The applied field is considered to be in the yz -plane and thus

represented by $h_{a2} = h_a \sin(\theta_h)$ and $h_{a3} = h_a \cos(\theta_h)$, where h_a is the magnitude and θ_h the angle from the z -axis. The betas represent resistance ratios used to calculate current in the STNO branch of the series circuit [10]. The following parameters will retain these values throughout this work: $\gamma = 0.0176$, $\lambda = 0.008$, $h_a = 300$, $\kappa = 45$, $\beta_{Rc} = 0.992$, $\beta_{\delta R} = 5.95 \times 10^{-4}$, $S_0 = \frac{8400}{4\pi}$.

Observe that the coupling term in (2) is a sum over all oscillators. This is indicative of all-to-all coupling which is represented by the symmetry group S_N .

3 INITIAL ANALYSIS

As an initial analysis, we make some simplifying assumptions about the system of equations. Starting with a system of $N = 2$ oscillators, we choose the following parameter values: $N_1 = N_2 = 0.5$, $N_3 = 0$, $\theta_h = 0$. This simplifies (2) to

$$\dot{z}_j = \frac{\gamma(1+i\lambda)}{1+\lambda^2} \left[ih_a z_j + ik \frac{1-|z_j|^2}{1+|z_j|^2} z_j - \mu I_{dc} z_j - \mu I_{dc} \beta_{\Delta R} \sum_{k=1}^N \frac{1-|z_k|^2}{1+|z_k|^2} z_j + 2\pi i S_0 \frac{z_j - z_j |z_j|^2}{1+|z_j|^2} \right]. \quad (3)$$

This form is convenient because it is invariant under the substitution $z = we^{i\phi}$, therefore each oscillator has S^1 symmetry. Combined with the system group representation (S_N), we now have $S_N \times S^1$ symmetry. We hope to leverage the work of [11], [12] concerning Hopf bifurcations with $S_N \times S^1$ symmetry.

To better describe the dynamics of this equation, XPPAUT is used to create a one-parameter bifurcation diagram in I_{dc} . In figure 1, we see stationary and limit-cycle steady-states plotted in x_1 vs I_{dc} coordinates, where x_1 is the real part of the first oscillator z_1 ($z_1 = x_1 + iy_1$). An artifact of the stereographic projection is that the ‘south pole’ of our sphere occurs at $|z| = \infty$. In this case, there is an equilibrium point exactly positioned at the south pole. The unstable limit-cycle intersects this equilibrium at $I_{dc} \approx 31.7$ in a Hopf Bifurcation (HB). The bifurcation diagram also unveils a problem with this portion of parameter space: the Hopf bifurcations are both sub-critical and spawn only unstable limit-cycles. Obviously, when building an oscillator it is important to have stable oscillations. This leads us to look at different values for N_1 and N_2 .

Making a small change in parameters ($N_1 = 0.6$, $N_2 = 0.4$), results in a new set of dynamics shown in figure 2. Again, this figure plots the real part of the first oscillator x_1 versus I_{dc} . Due to symmetry in the system, the bifurcation diagram is symmetric across $x_1 = 0$. There are now many more equilibria and limit cycles as well as Saddle Node (SN) bifurcations. Additionally, we now have stable oscillations in the system. Furthermore,

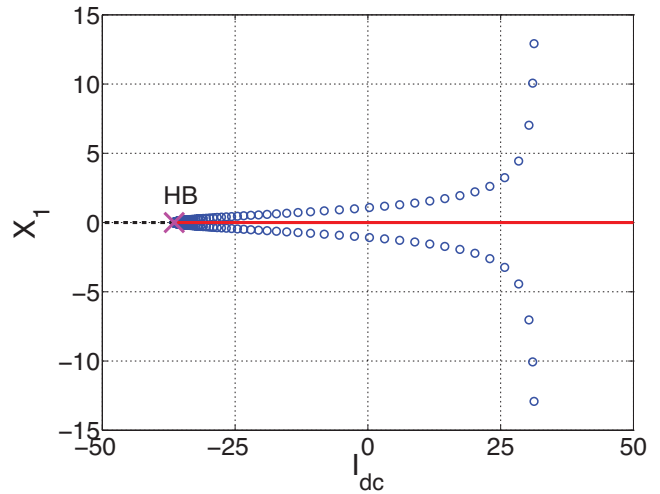


Figure 1: One parameter bifurcation diagram $\theta_h = 0$, $N_1 = N_2 = 0.5$. Red solid lines = stable equilibrium, dashed black lines = unstable equilibrium, open circles = max/min of unstable limit cycle, closed circle = max/min of stable limit cycle.

the majority of the stable oscillations are synchronized. However, as in the $N_1 = N_2 = 0.5$ case, $\|z\| = \infty$ is a stable equilibrium in the oscillating range and thus attracts many initial conditions.

As we continue to increase N_1 , the region of I_{dc} with stable oscillations continues to expand. At the maximum value $N_1 = 1$, we see large regions of I_{dc} with stable oscillations, however both the synchronized and

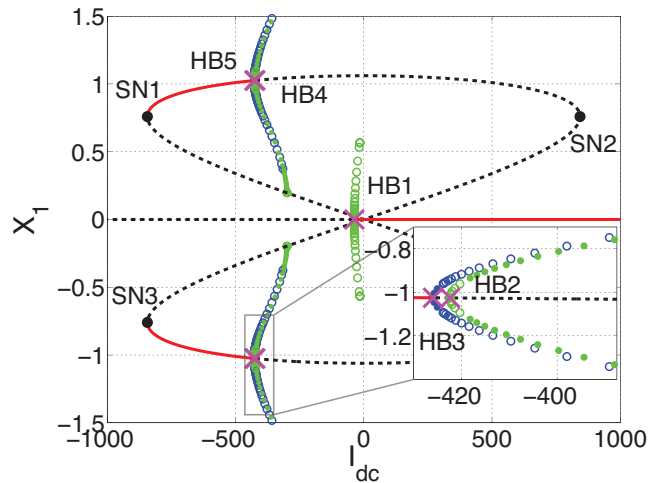


Figure 2: One parameter bifurcation diagram $\theta_h = 0$, $N_1 = 0.6$, $N_2 = 0.4$. Red solid lines = stable equilibrium, dashed black lines = unstable equilibrium, open circles = max/min of unstable Limit Cycle (LC), closed circle = max/min of stable LC, green = synchronized LC, blue = OoP LC.

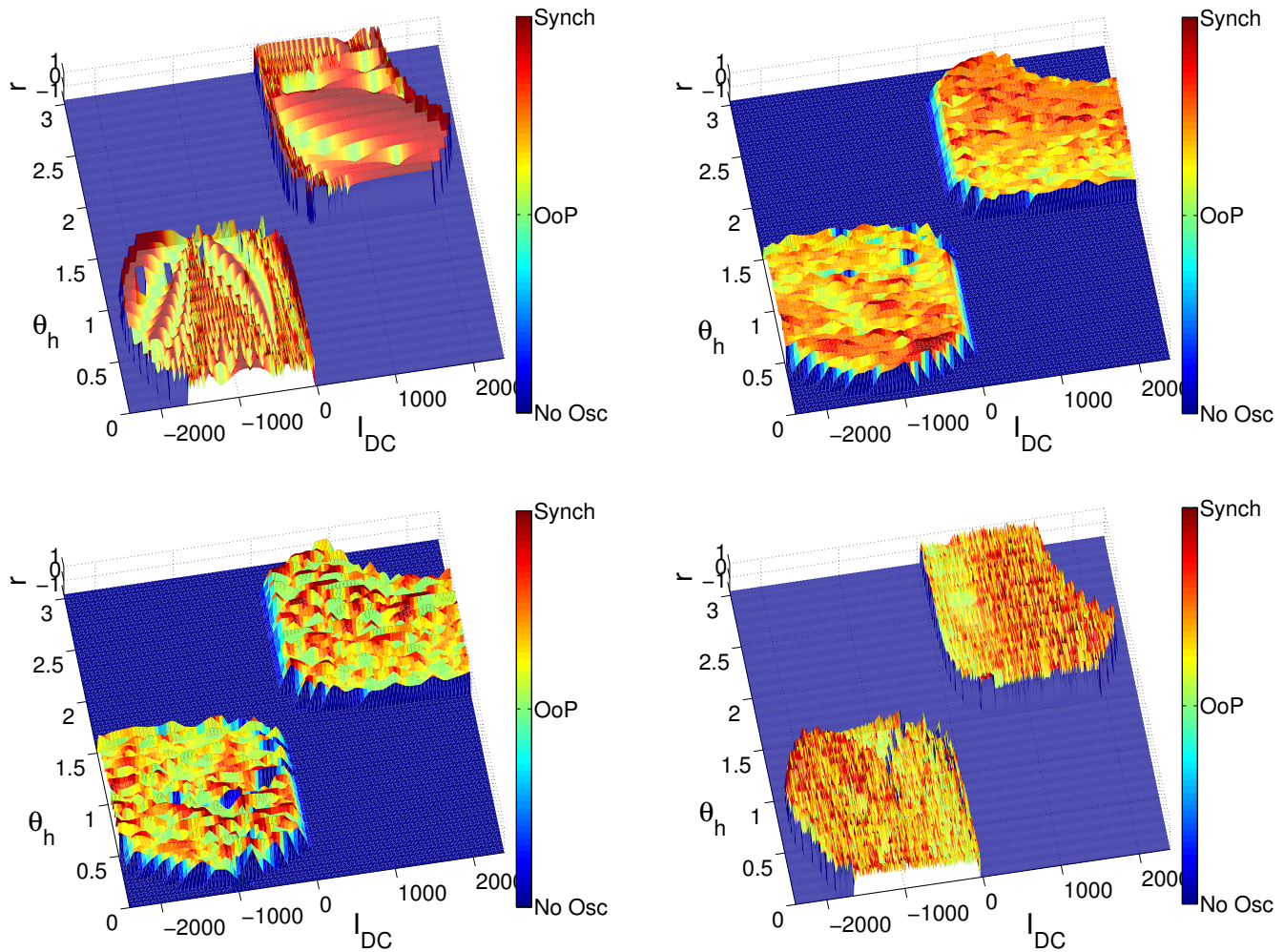


Figure 3: Coherence calculated in two parameter space: θ_h vs I_{dc} . (Top left) $N = 2$. (Top right) $N = 3$. (Bottom left) $N = 4$. (Bottom right) $N = 5$.

out-of-phase solutions are stable. This bistability indicates that the system is sensitive to initial conditions and thus basins of attraction must be calculated to fully characterize the system. However, even the $N = 2$ system has initial conditions in four dimensions. Due to this dimensionality, both the calculation and visualization of basins of attraction are non-trivial problems.

4 COHERENCE CALCULATION

A system of oscillators can be characterized by its coherence

$$r = \frac{1}{N} \left| \sum_{k=1}^N e^{i\phi_k} \right|, \quad 0 \leq r \leq 1. \quad (4)$$

Here ϕ_k is the phase of the k th-oscillator and N is the number of oscillators. A coherence $r = 1$ indicates phase-synchronization while $r = 0$ occurs for equal

phase spacing (splay-phase) of the oscillators. The spectrum therein can be considered a measure of phase synchronization. Figure 3 is generated by discretizing the two dimensional parameter space (θ_h, I_{dc}) on a rectangular grid, generating random initial conditions for each grid point, integrating to steady-state, and then calculating coherence. Points with no oscillations are arbitrarily set to -1 and appear blue in the figure. While this technique does not completely describe the system, it should show any regions where the synchronized state's basin of attraction dominates. In fact, looking at $N = 2$ and especially $\theta_h > \pi/2$, a significant region of synchronization emerges.

As N is increased, the synchronized grid points become intermixed indicating competing basins of attraction from Out-of-Phase (OoP) solutions. The general trend is that increasing the number of oscillators N appears to decrease the likelihood of finding initial condi-

tions that result in synchronization.

5 DISCUSSION

Given the prevalence for bistability in regions of oscillation, basins of attraction must be calculated to completely determine conditions for synchronization. However, for the relatively simple case of $N = 2$ this requires working in and visualizing a four dimensional space. In future work we intend to determine basins of attraction by calculating the invariant manifolds. Ideally the work would then be extended to larger N , but the difficulties associated with operating in 6+ dimensions may prove prohibitive.

Once the small N cases are fully described, we must turn our analyses to larger networks of oscillators. The initial results presented here suggest that it may become more difficult to determine conditions for synchronization as the number of STNOs N increases. Consequently we must develop methods of analysis that scale well with increasing N . One such approach is to leverage the coupling symmetry S_N and previous work [11], [12] to analyze the symmetry-breaking Hopf bifurcations. These principles allow us to determine the existence and stability of all Hopf-born non-synchronous limit-cycles in the neighborhood of the Hopf from whence they came. By focusing on Hopfs that occur on common equilibrium, the analysis will scale well with N while capturing all periodic solutions with maximal isotropy.

REFERENCES

- [1] A. Wickenden, C. Fazi, B. Huebschman, R. Kaul, A. Perrella, W. Rippard, and M. Pufall, *Spin torque nano oscillators as potential terahertz (thz) communication devices*. Technical Report, DTIC Document, 2009.
- [2] J. Persson, Y. Zhou, and J. Akerman, “Phase-locked spin torque oscillators: Impact of device variability and time delay,” *J. Appl. Phys.*, vol. 101, no. 9, pp. 09A503–09A503, 2007.
- [3] D. Li, Y. Zhou, C. Zhou, and B. Hu, “Global attractors and the difficulty of synchronizing serial spin-torque oscillators,” *Phys. Rev. B*, vol. 82, no. 14, p. 140407, 2010.
- [4] L. Berger, “Emission of spin waves by a magnetic multilayer traversed by a current,” *Phys. Rev. B*, vol. 54, no. 13, pp. 9353–9358, Oct 1996.
- [5] G. Bertotti, I. Mayergoyz, and C. Serpico, “Analytical solutions of landau-lifshitz equation for precessional dynamics,” *Phys. B*, vol. 343, no. 1-4, pp. 325–330, 2004.
- [6] M. d’Aquino, “Nonlinear magnetization dynamics in thin-films and nanoparticles,” Ph.D. dissertation, Università degli Studi di Napoli Federico II, Naples, Italy, 2004.

- [7] T. Gilbert, “A phenomenological theory of damping in ferromagnetic materials,” *IEEE T. Magn.*, vol. 40, no. 6, pp. 3443–3449, 2004.
- [8] J. C. Slonczewski, “Current-driven excitation of magnetic multilayers,” *J. Magn. Magn. Mater.*, vol. 159, no. 1-2, pp. L1–L7, 1996.
- [9] J. Turtle, K. Beauvais, R. Shaffer, A. Palacios, V. In, T. Emery, and P. Longhini, “Gluing bifurcations in coupled spin torque nano-oscillators,” *Journal of Applied Physics*, vol. 113, no. 11, p. 114901, 2013.
- [10] J. Grollier, V. Cros, and A. Fert, “Synchronization of spin-transfer oscillators driven by stimulated microwave currents,” *Phys. Rev. B*, vol. 73, 2006.
- [11] A. P. S. Dias and R. C. Paiva, “Hopf bifurcation with S_3 -symmetry,” *Portugaliae Mathematica*, vol. 63, no. 2, p. 127, 2006.
- [12] A. P. S. Dias and A. Rodrigues, “Hopf bifurcation with S_N -symmetry,” *Nonlinearity*, vol. 22, no. 3, p. 627, 2009.